Journal of Power Sources 520 (2022) 230804

Contents lists available at ScienceDirect

Journal of Power Sources

journal homepage: www.elsevier.com/locate/jpowsour

Improvement of safe bromine electrolytes and their cell performance in H_2/Br_2 flow batteries caused by tuning the bromine complexation equilibrium

Michael Küttinger [a,b,*], Raphaël Riasse [a], Jakub Wlodarczyk [c], Peter Fischer [a], Jens Tübke [a,b]

[a] Department of Applied Electrochemistry, Fraunhofer Institute for Chemical Technology ICT, Joseph-von-Fraunhofer-Strasse 7, D-76327, Pfinztal, Germany
[b] Institute for Mechanical Process Engineering and Mechanics, Karlsruhe Institute of Technology KIT, Strasse am Forum 8, D-76131, Karlsruhe, Germany
[c] Institute of Computational Physics (ICP), Zurich University of Applied Sciences (ZHAW), Wildbachstrasse 21, CH-8400, Winterthur, Switzerland

HIGHLIGHTS

- Evaluation of bromine posolytes with complexing agents (BCA) for energy storage.
- Investigation of Br_2 transfer mechanism between aqueous electrolyte and fused salt.
- Successful development of electrolyte by intervention in complexation reaction.
- Reduced influence of BCA cation on PFSA membrane performance and cell performance.
- Increase of the useable electrolyte capacity from 53.9 Ah L^{-1} to 179.6 Ah L^{-1}.

ARTICLE INFO

Keywords:
Redox flow batteries
Bromine posolytes
Bromine complexing agent
Complexation reaction
Storage capacity
Cycling performance

ABSTRACT

Hydrogen bromine redox flow batteries utilize bromine electrolytes in their positive half cell, offering capacities larger than 100 Ah L^{-1}. Addition of quaternary ammonium compounds, so-called bromine complexing agents (BCA), may increase safety as they reduce the vapour pressure of bromine in the posolyte. However, they have not been applied so far. They (a) interact with perfluorosulfonic acid membranes leading to significant reduction of membrane conductivity and (b) they form a low conductive ionic liquid with polybromides, leading to high overvoltage if the formation happens at the electrode. In this work a solution to this problem is proposed by an excess addition of Br_2 to these electrolytes. The excess bromine leads to a permanent bromine fused salt phase in the tank. Bromine formed in the cell stays in the aqueous phase and bromine transfer between the two phases happens in the tank. Transfer of Br_2 without the transfer of $[BCA]^+$ cations exists between the phases, while $[C2Py]^+$ cations remain in the fused salt and do not influence cell performance. For the first time a posolyte capacity of 179.6 Ah L^{-1} based on 7.7 M hydrobromic acid with BCA is achieved compared to previous investigations with e.g. 53.9 Ah L^{-1}.

1. Introduction

Hydrogen bromine redox flow batteries (H_2/Br_2-RFB) used as stationary energy storage solutions have nowadays entered to the commercialisation stage [1–4]. Large-scale H_2/Br_2-RFB storage (500 kW/5 MWh) has the potential to be competitive with lithium ion batteries and fossil fuel-based energy generating technologies in the future thanks to storage costs between \$0.034 kWh^{-1} and \$0.074 kWh^{-1} [1,4]. H_2/Br_2-RFB uses a negative hydrogen half cell, comparable to PEM fuel cells [4] in combination with a bromine half cell, which is fed with liquid aqueous hydrobromic acid (HBr) containing bromine (Br_2) [3]. The positive half cell reaction of the Br_2/Br^- redox couple [3,5,6] occurs according to Eqn. (1) [7,8].

$$2\ Br^- \underset{\text{DISCHARGE}}{\overset{\text{CHARGE}}{\rightleftharpoons}} Br_2 + 2\ e^- \quad E_0 = 1.087\ V \tag{1}$$

Organic quaternary ammonium compounds act as bromine complexing agents (BCAs) to lower the vapour pressure of Br_2 and lead to safer bromine electrolytes [9–16]. However, the application of BCAs in

* Corresponding author. Department of Applied Electrochemistry, Fraunhofer Institute for Chemical Technology ICT, Joseph-von-Fraunhofer-Strasse 7, D-76327, Pfinztal, Germany.
E-mail address: michael.kuettinger@gmx.de (M. Küttinger).

https://doi.org/10.1016/j.jpowsour.2021.230804
Received 1 June 2021; Received in revised form 13 October 2021; Accepted 21 November 2021
Available online 1 December 2021

the bromine half cell leads to a reduced conductivity of the deployed perfluorosulfonic acid (PFSA) membrane [17,18] and causes a decrease of electrolyte conductivity [18]. In this work the BCA is transferred into a second electrolyte phase outside of the cell, by influencing the BCA solubility equilibrium. It is intended to prevent contamination of the cell by $[BCA]^+$ cations while maintaining their effect in lowering bromine volatility.

1.1. State of the art

Br_2 is hardly soluble in water [19–21], but forms well soluble polybromides with bromide (Br^-) such as tribromide Br_3^-, pentabromide Br_5^- and heptabromide Br_7^- (Eqn. (2)) [8,22–26]:

$$Br^-(aq) + n\ Br_2(l) \rightleftharpoons Br_{2n+1}^-(aq) \text{ with } n = 1, 2, 3 \quad (2)$$

In BCA-free electrolytes capacities up to 179.6 Ah L^{-1} are reached [27], but cause unsafe bromine vapour in the tank. The theoretical capacity Q of the electrolyte bases on a cyclable HBr concentration of Δc (HBr) = 6.7 M [27]. It is calculated by applying the Faraday law (Eqn. (3)) including concentration changes of the redox active species, the Faraday constant F and the stoichiometric factor z.

$$Q = z \cdot F \cdot \Delta c(HBr) = 1 \cdot 96485\ As\ mol^{-1} \cdot 6.7\ mol\ L^{-1} \cdot (3600\ s\ h^{-1})^{-1} = 179.6\ Ah\ L^{-1} \quad (3)$$

Quaternary ammonium compounds such as 1-methyl-1-ethylpyrrolidin-1-iumbromide ([MEP]Br) or 1-methyl-1-ethylmorpholin-1-iumbromide ([MEM]Br) are used in zinc/bromine-RFB and vanadium/bromine-RFB [9,15,28–32] to bind bromine in solution [9,12,13,15,16]. Further BCA types have been investigated and show similar properties [11,13,15,29,33–35]. While the bromide salts of $[BCA]^+$ cations solubilise in aqueous bromide solutions (aq), polybromide salts precipitate and form a liquid fused salt phase (fs) following Eqn. (4) [11,15]. The fused salt phase (fs) of $[BCA]^+$ cations has properties of an ionic liquid [11,15,36].

$$[BCA]^+(aq) + Br_{2n+1}^-(aq) \leftrightarrows [BCA]Br_{2n+1}(aq) \leftrightarrows [BCA]Br_{2n+1}(fs) \quad (4)$$

Another BCA compound, 1-ethylpyridin-1-ium bromide [C2Py]Br [11,17,18,34,37,38], reduces the amount of Br_2 in aqueous electrolytes by at least 90 mol% compared to the absolute amount of bromine (3.35 M Br_2) at state of charge (SoC) 100% [11,18]. A safe electrolyte is achieved by reaching low Br_2 concentration in the aqueous phase when using $[C2Py]^+$ cations [18,34,37]. However, the positively charged cations in the aqueous electrolyte phase adversely affect the cell performance: (1) During charge operation, bromine and polybromides are formed in the positive half cell. In contact with the $[C2Py]^+$ cations, a formation and accumulation of fused salt with low electrolyte conductivity (κ) of $\kappa < 98$ mS cm^{-1} in the bromine half cell occur and lead to high overvoltage [18]. In parallel, (2) $[C2Py]^+$ cations interact with PFSA membranes in H_2/Br_2-RFB, as described by different authors [17,18,39–43]. The hydrophobic and dissolved $[BCA]^+$ cation forms an addition bonding with the deprotonated sulphonate group in the membrane and dries the membrane channels from water [43]. The transport of protons in the PFSA is limited [44]. Porous polyvinylidendifluorid-SiO_2 (PVDF-SiO_2) separators without ionic exchange functionalities reduce the effect on the membrane [17]. However, the formation of low conductive fused salt in the positive half cell is not prevented [15,18].

Both processes lead to a maximum capacity utilization of 30% of a 7.7 M HBr/1.11 M $[C2Py]^+$ electrolyte (53.9 Ah L^{-1}) [18], compared to BCA-free posolytes ($HBr/Br_2/H_2O$) with maximum capacities of 179.6 Ah L^{-1} [27]. The $[BCA]^+$ cation concentration shall be as low as possible in the bromine half cell during operation in order to prevent its negative effect on the cell performance [18].

1.2. Work plan

The focus of this work is to develop safe and powerful bromine electrolytes based on [C2Py]Br. In order to prevent $[C2Py]^+$ cations to exist in the aqueous phase of the positive bromine half cell, the ambition is to intervene in the solubility equilibrium of the bromine complexation in Eqn. (4). By introducing an excess amount of Br_2 at SoC 0%, nearly all of the $[BCA]^+$ cations shall be transferred into the fused salt phase, following Eqn. (4), resulting in a decrease of the $[BCA]^+$ cations concentration in the aqueous phase. This idea is implemented using an electrolyte with a high theoretical energy density of 179.6 Ah L^{-1} [27]. The excess amount of Br_2 is available within the entire SoC range (Fig. 1a) and is not used for energy storage, but enables a passive and safe bromine storage during the cell operation. The approach is shown in Fig. 1b:

In this work, three electrolyte mixtures with different amounts of bromine at SoC 0% (+0.00 M; +1.68 M; +2.51 M Br_2) (Fig. 1), which are hereafter referred as "series no. 1, 2 and 3" are investigated on composition and cell performance. Series no. 1 defines the standard case in literature [18] without Br_2 in the electrolyte at SoC 0%. The addition of Br_2 is intended to reduce the $[C2Py]^+$(aq) concentration in series no. 2

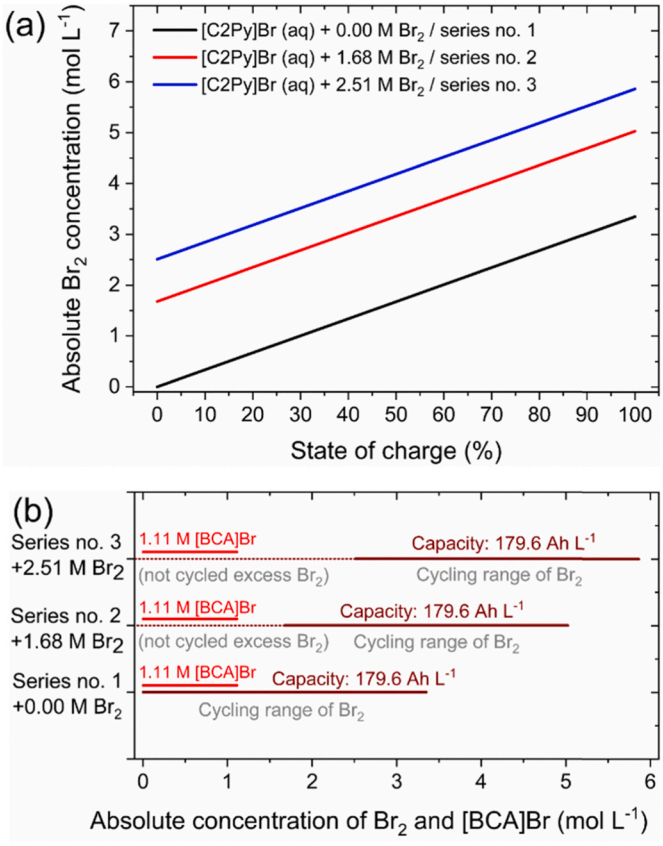

Fig. 1. (a) Absolute Br_2 concentration in the electrolyte samples in this work depending on the state of charge (SoC) and depending on different initial Br_2 excess concentrations at SoC 0% (series no. 1 - + 0.00 M Br_2, series no. 2 - + 1.68 M Br_2 and series no. 3 - + 2.51 M Br_2). Concentrations are calculated by means of Eqn. (6). (b) Scheme comparing the absolute Br_2 concentration with the absolute $[BCA]^+$ cations concentration of 1.11 M in this work. The excess amounts of Br_2 at SoC 0% shift the used concentration range of Br_2 for a useable capacity (Q) of 179.6 Ah L^{-1} to higher absolute Br_2 concentrations (brown lines), while the excess amounts are not involved in the cell reaction during operation (brown dotted lines). The idea is to complex the $[BCA]^+$ cations (red lines) by the excess Br_2 (brown dotted lines). The excess amounts of Br_2 are not used for energy storage but for transferring and storing $[BCA]^+$ cations into the fused salt. (For interpretation of the references to colour in this figure legend, the reader is referred to the Web version of this article.)

and 3, as fractions of the Br_2 concentration are only used to bind Br_2 (Fig. 1b) in the fused salt phase. During battery operation, the range of absolute Br_2 concentrations shifts to higher bromine concentrations (Fig. 1a) or higher ratio between absolute bromine amounts and absolute $[BCA]^+$ amounts (Fig. 1b) in the electrolytes.

The absolute concentrations of HBr and Br_2 based on the SoC and the excess concentrations of Br_2 c(Br_2, excess) in the electrolyte are defined in Eqn. (5) and Eqn. (6).

$$c(HBr_{absolute}) = 6.7\ \ M \cdot (1 - SoC) + 1.0\ \ M \tag{5}$$

$$c\left(Br_{2,\ absolute}\right) = 3.35\ \ M\ \cdot SoC\ \ + c\left(Br_{2,\ excess}\right) \tag{6}$$

The interference in the equilibrium according to Eqn. (4) is comprehensively investigated for all performance-relevant parameters in the bromine half cell of a H_2/Br_2-RFB with a PFSA membrane (Nafion117): (i) concentration of $[C2Py]^+$ in the aqueous solution, (ii) bromine concentration and polybromide distribution in the aqueous phase, (iii) conductivity of the aqueous solution, (iv) influence of the parameters in (i, ii and iii) on cell performance and (v) change in the composition of the fused salt. The research article discusses three different bromine transfer mechanisms between the two electrolyte phases in the results.

2. Experimental and methods

A detailed version of the chapter "Experimental and methods" is available in the Electronic Supplementary Information (ESI).

2.1. Chemicals and composition of the electrolytes

Electrolyte solutions consist of HBr, water and Br_2. The used BCA [C2Py]Br is synthesised from Refs. [13,45,46]. The synthesis of [C2Py]Br is confirmed by ^{1}H NMR and ^{13}C NMR analysis by comparison with literature [46,47] (ESI). In all electrolyte samples 1.11 M (absolute) [C2Py]Br is available within the whole SoC range. The absolute concentrations of HBr related to the SoC of the electrolyte are defined as follows: SoC 0% with 7.7 M HBr and SoC 100% with 1 M HBr (Eqn. (5)). The concentrations of Br_2 in the electrolytes depend on the chosen excess amount of Br_2 at SoC 0% in series no. 1, 2 and 3 and are shown in Table 1 and calculated for any SoC and excess amounts of Br_2 following Eqn. (6).

For ex situ measurements, electrolyte samples are mixed for all three electrolyte series with a volume (V) of V = 30 mL for SoC 0, 10, 20, 30, 33, 40, 50, 60, 66, 70, 80, 90 and 100%. Detailed absolute concentrations are shown in Tables S–2 in the ESI. The electrolyte (V = 90 mL) used for cell test cycling is prepared at SoC 100% (Table 1).

2.2. Concentration of [C2Py]Br in aqueous electrolyte solution

Concentrations of $[C2Py]^+$(aq) in equilibrated aqueous phase are investigated by Raman spectroscopy from aqueous electrolyte samples for all three electrolyte series and at all 13 SoCs. Details on the Raman spectrometer equipment are shown in the ESI. $[C2Py]^+$ leads to a strong single Raman peak signal at a Raman shift ($\tilde{\nu}$) $\tilde{\nu}$ = 1029 cm^{-1} [48–50]. Comparison of the peak area with the peak area of a reference electrolyte leads to $[C2Py]^+$(aq) concentrations. Detailed information is shown in the ESI.

Table 1
Bromine concentrations defined for three different electrolyte mixtures at SoC 0% and SoC 100%.

Electrolyte mixture	Concentration of bromine Br_2/M	
	SoC 0%	SoC 100%
Electrolyte series no. 1	0.00	3.35
Electrolyte series no. 2	1.68	5.03
Electrolyte series no. 3	2.51	5.86

2.3. Bromine concentrations in aqueous electrolyte solution and fused salt

Bromine concentrations in the aqueous electrolytes are determined for all three electrolyte series and chosen SoCs by means of linear chronoamperometry at a rotating disk electrode on a vitreous carbon electrode. Starting from the open circuit potential the potential is reduced to −1.0 V vs. Ag/AgCl/KCl(sat.) with a scan rate of −40 mV s^{-1}. Current response shows a constant limiting discharge current for low potentials, which is proportional to the Br_2 concentration by Levich equation [51–55]. Concentration of Br_2 are calculated from limiting currents following Eqn. (7) ([c(Br_2)] = mol L^{-1}, [I_{lim}] = mA). Calibration leads to a coefficient m equal to 3.424•10^{-3} mol L^{-1} mA^{-1}:

$$c(Br_2(aq)) = m \cdot I_{lim} \tag{7}$$

Concentrations of Br_2 in fused salt c(Br_2(fs)) are calculated from c(Br_2(aq)) and volumes of aqueous phase V(aq) and of corresponding fused salt V(fs) shown in the ESI.

2.4. Fractions of Br_2 in different polybromides

The actual polybromide composition in the electrolyte phases is defined by the fractions x(Br_2 in Br_{2n+1}^-) showing the distribution of Br_2 on the different polybromides Br_3^-, Br_5^- and Br_7^- as explained in Ref. [27]. The distributions are examined by means of Raman spectroscopy in both phases for all three series and all chosen SoCs ex situ. All polybromides and Br_2 show peaks with at characteristic Raman shifts between 120 $\leq \tilde{\nu} \leq$ 340 cm^{-1} for symmetrical and antisymmetrical stretching vibration of the polybromides, which are listed in the ESI and in Refs. [27,36,38,56–59]. Data on the setup of the Raman spectrometer and the analysis procedure including scientific background on polybromide investigation are presented in detail in the ESI. Peak areas at characteristic Raman shifts of the symmetrical stretching oscillation are determined by fitting. Fitting results are shown for four examples in the ESI (Figure S-8 to S-11). Areas under the symmetric stretching vibration peaks assigned to Br_3^-, Br_5^-, and Br_7^- are related to the sum of all peak areas of symmetric vibrations to achieve fractions x(Br_2 in Br_{2n+1}^-) on polybromides [27].

2.5. Conductivities of aqueous electrolytes

Electrolytic conductivities of aqueous electrolyte solutions (series no. 1 to 3 at all chosen SoCs) are determined in a calibrated conductivity cell at $\vartheta = 23 \pm 1$ °C by impedance spectroscopy. Conductivity calculations and the determination of the cell constant are explained in the ESI.

2.6. Cycling tests and H_2/Br_2-RFB test cell

Cell tests are performed by galvanostatic cycling with a current density of ±50 mA cm^{-2} or ±100 mA cm^{-2} in a H_2/Br_2-RFB single cell to evaluate cycling performance of the three electrolytes. Starting from a SoC 100% the cell test operates with a discharge process followed by a charge process. SoC values for the electrolytes after discharge operation and after charge operation are calculated from the cell current and the discharge/charge time for each cycle by summing up the converted charge Q during the experiment (Eqn. (8)). The SoC after charge or discharge SoC (t_2) bases on the SoC (t_1) before charge or discharge operation, and the converted amount of charges Q (Eqn. (8)). At the beginning of the experiments SoC (t_1) is 100%:

$$SoC\ \ (t_2) = \frac{Q}{z\ \ F\ \ 6.7\ \ M\ \ HBr\ \ \cdot 0.09\ \ L} + SoC\ \ (t_1)$$
$$= \frac{\int_{t_1}^{t_2} I(t)\ \ dt}{z \cdot F\ \ \cdot 6.7\ \ M\ \ HBr\ \ \cdot 0.09\ \ L} + SoC(t_1) \tag{8}$$

A Nafion117 membrane with a geometrical active area of 40 cm^2 and coated single-sided with a Pt/C catalyst for the H_2 reactions is used in the cell. The Nafion117 has a thickness of 175 μm in its dry state [60,61] and is applied due to its good proton transport property [62,63]. Due to its thickness, it reduces the crossover of water, polybromides and bromine, as well as H_2 [4,64], and is also used for that reason in other gas/liquid systems such as vanadium-air fuel cells [65,66] or methanol fuel cells [67,68]. Since it is coated with Pt catalyst on one side, it cannot be pre-treated in H_2O_2/H_2SO_4 solutions under boiling, as is the case of Nafion membranes used in a liquid/liquid-RFB like the all-vanadium RFB [60,61] and is only placed for 24 h in pure water. A graphite felt electrode is embedded in a flow frame of the positive half cell. Further material and cell information are provided in the ESI. The hydrogen half cell is operated in a non-recyclable flow through mode with a flow rate of 100 mL min^{-1} (dry) during charge and discharge operation. The aqueous electrolyte is pumped continuously through the positive half cell felt with a flow rate of 30 mL min^{-1}, while the fused salt remains in the tank. The two phase electrolyte is stored in a sealed glass tank. The cell voltage $E_{Cell\ i \neq 0}$ under operation, the redox potential of the electrolyte $\varphi(Br_2/Br^-)_{redox}$ versus the normal hydrogen electrode (NHE), half cell potentials of the positive bromine half cell $\varphi(Br_2/Br^-)_{i \neq 0}$ vs. NHE and the negative hydrogen half cell potential $\varphi(H^+/H_2)_{i \neq 0}$ vs. NHE are determined in parallel during cycling experiments. The setup is shown in the ESI. Between discharge/charge operation during the cycling test the ohmic cell resistances are investigated by means of galvanostatic electrochemical impedance spectroscopy (EIS).

3. Results and discussion

3.1. Reduction of $[C2Py]^+$ cations in the aqueous electrolyte phase

To achieve a transfer and storage of $[C2Py]^+$ into the fused salt phase within the entire SoC range, an excess amount of Br_2 is added and should shift the complexation equilibrium (Eqn. (4)) to the fused salt side, causing a large fraction of Br_2 and also of $[C2Py]^+$ to pass from the aqueous phase into the fused salt. $[C2Py]^+$(aq) concentrations in aqueous electrolytes are investigated for chemical equilibrium between the two phases by means of Raman spectroscopy and presented in Fig. 2.

For all electrolyte series, the concentrations decrease with increasing SoC, which is related to the rising absolute Br_2 concentration based on the electrochemical half cell reaction (Eqn. (1)). Especially for series no. 1 the intense transfer of $[C2Py]^+$ from the aqueous phase to the fused salt phase (Eqn. (4)) is recognisable. The strongest decrease of the $[C2Py]^+$(aq) concentration for all series is in the range SoC <40%.

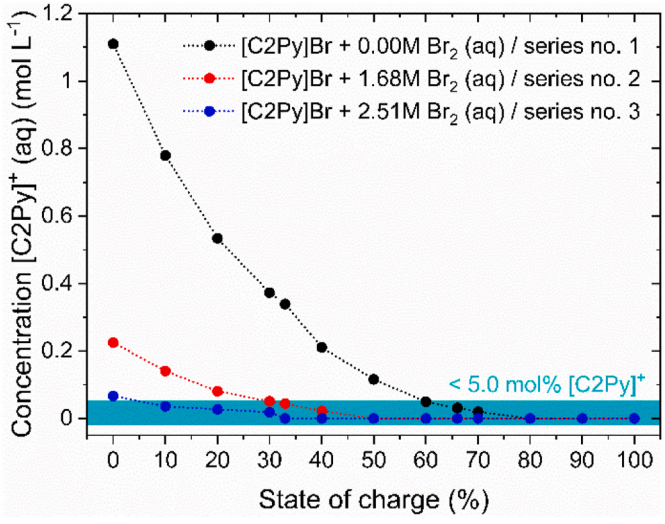

Fig. 2. Concentration of $[C2Py]^+$ cations in the aqueous electrolyte phase as a function of SoC for electrolyte series no. 1 (+0.00 M Br_2), no. 2 (+1.68 M Br_2) and no. 3 (+2.51 M Br_2) including concentration range with $[C2Py]^+$ concentration lower than 5.0 mol% related to the original concentration of 1.11 M $[C2Py]^+$ (blue area). (For interpretation of the references to colour in this figure legend, the reader is referred to the Web version of this article.)

The concentration of $[C2Py]^+$(aq) in aqueous electrolyte phase is significantly reduced by the excess bromine in series no. 2 and 3, especially for SoC <50% (Fig. 2). At SoC 0% already only 0.23 M $[C2Py]^+$(aq) (20.7 mol% vs. 1.11 M BCA) are left in series no. 2, while for series no. 3 only 0.07 M $[C2Py]^+$ in aqueous solution (6.3 mol% vs. 1.11 M BCA) are measured. The excess of Br_2 leads to a preferred formation and transfer of $[C2Py]Br_{2n+1}$(fs) into the fused salt causing a decrease of $[C2Py]^+$(aq) following Eqn. (4).

For higher SoCs $[C2Py]^+$ concentrations are too low to be detected by Raman Spectroscopy. While for series no. 1 $[C2Py]^+$(aq) is not detected for SoC ≥ 70%, it is undetectable in series no. 2 for SoC ≥ 60% and in series no. 3 for SoC ≥ 50%. Rising amounts of excess Br_2 lead to wider BCA-free SoC ranges in that way. In these SoC ranges the aqueous phase is approximately free of $[C2Py]^+$ cations.

For series no. 3, c($[C2Py]^+$) is below 5 mol% referred to the maximum possible concentration of 1.11 M for 95% of the electrolytes' operation range (SoC 5–100%), which is close to the objective of a $[C2Py]^+$-free aqueous phase and expected to enhance cell performance.

3.2. Br_2 concentration and polybromide composition in the aqueous electrolyte phase

3.2.1. Bromine concentrations and safety of electrolytes

For reaching high current densities, normally large Br_2 concentrations are required in the bromine half cell, but in parallel a safe electrolyte bases on low amounts of Br_2 in the aqueous phase. A compromise would be to reach moderate Br_2 concentrations during the operation within the SoC range. The Br_2 concentration in the aqueous phase is influenced due to the solubility equilibrium (Eqn. (4)). Br_2 concentrations for all three electrolyte series within the entire SoC range are investigated from equilibrated aqueous phases and depicted in Fig. 3a and Table 2.

In general, Br_2 concentrations increase in the aqueous solution within the entire SoC range (Fig. 3a) for series no. 2 and no. 3 due to rising Br_2 concentrations and the excess of Br_2 compared to the electrolyte samples without excess of Br_2 in series no. 1. The concentrations in no. 2 and 3 are much higher than in no. 1 as the excess amounts of Br_2 are not bound strong enough due to a lack of $[C2Py]^+$(aq) to achieve Br_2 concentrations of series no. 1 with c(Br_2) ≤ 0.28 M. Maximum bromine concentrations $c(Br_2)_{max}$ are reached at specific SoC between SoC 70% and SoC 90% and have values between 0.28 and 1.26 M Br_2 (Table 2, column 2 and 3). However, despite the large concentrations of Br_2 up to 1.26 M in the aqueous phase of series no. 2 and 3, more than 74 mol% of the Br_2 passes into the fused salt related to absolute bromine concentrations as shown in Table 2 in column 4 and 5.

No definition for neither maximum concentration of Br_2 nor their vapour pressures concerning safety parameters of the system are mentioned in the literature so far. This is why measurements in this study are based on concentrations only. However, large fractions of the Br_2 are bound in fused salt and the $[C2Py]^+$ cations are mostly transferred into the fused salt. The BCA complies the target to reduce the Br_2 concentration in the aqueous phase. It remains to investigate if these electrolytes can still be classified as "quasi-safe", which depends on accident scenarios, which shall be discussed elsewhere.

3.2.2. Bromine solubility equilibrium at high SoC

Polybromides and $[C2Py]^+$ cations form the fused salt phase due to the solubility equilibrium (Eqn. (4)). However, for SoC >70% and depending on the electrolyte series, it possible to investigate that the solubility equilibrium Eqn. (4) does not sufficiently describe the processes of Br_2-transfer between the aqueous and the fused salt from the

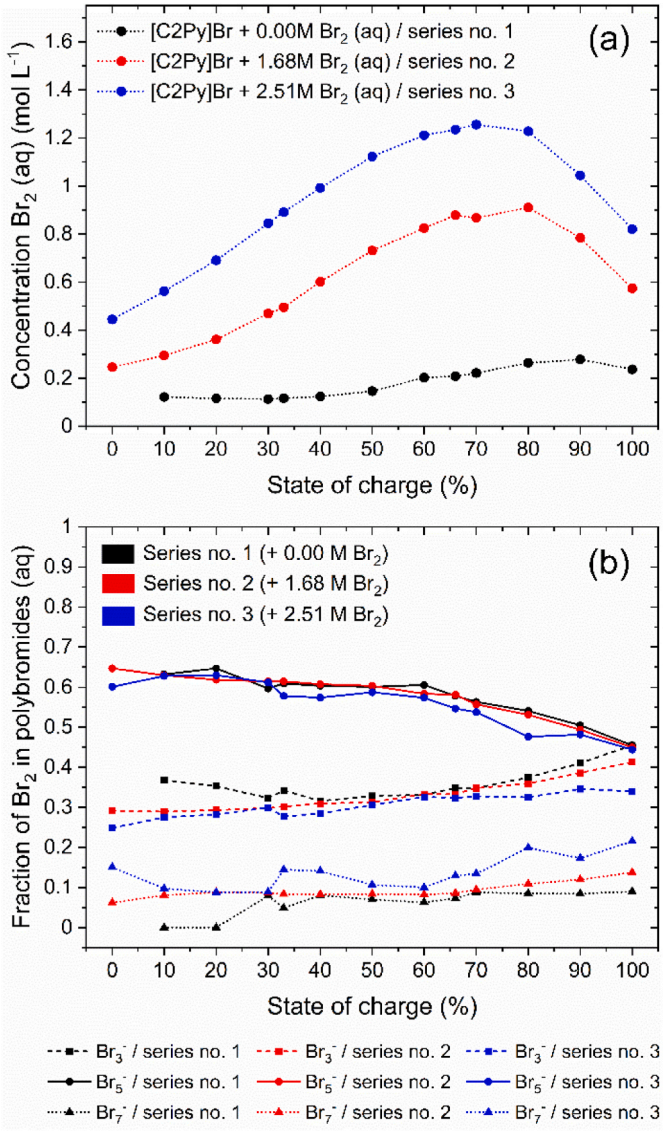

Fig. 3. Bromine content in the aqueous electrolyte phase for electrolyte series no. 1, 2 and 3: (a) concentration of bromine in aqueous electrolyte solution and (b) distribution of bromine in tri-, penta- and heptabromide in the aqueous electrolyte solutions as a function of SoC and electrolyte series no. 1 to 3 at $\vartheta = 23 \pm 1$ °C.

results in Sections 3.1 and 3.2.1.

It is recognized, that from the SoC with highest concentration $Br_2(aq)_{max}$ (Table 2) to SoC 100% the solubility of Br_2 is limited in the aqueous phase for all series. Br_2 concentrations decrease in this SoC range (Fig. 3a) while the absolute Br_2 concentrations still rise (Fig. 1a). In parallel all aqueous electrolyte phases in this SoC range are free of $[C2Py]^+$(aq). Br_2 is transferred into the fused salt, leading to falling concentration of Br_2 in the aqueous phase, but a transfer according to Eqn. (4) is not possible to take place.

For high SoC, the Br_2 passes into the fused salt, as its solubility in the BCA-free aqueous phase is limited, which is not the case in the fused salt. From SoC >70% the concentration of HBr(aq) are lower than 3.01 M and not sufficient to form polybromides from all Br_2 molecules in aqueous solution. In parallel the fused salt absorbs Br_2 from the aqueous phase. The shown solubility effect is comparable to BCA-free electrolytes in this SoC range, as it has been discussed in Ref. [27]. Therefore, Br_2 reaches saturation in the aqueous phase and is forced to pass directly into the fused salt following Eqn. (9).

$$Br_2(l) + \ Br_{2n-1}^-(fs) \rightleftharpoons \ Br_{2n+1}^-(fs) \tag{9}$$

3.2.3. *Polybromide distribution in the aqueous phase*

The influence of the excess bromine on the distribution of Br_2 on the polybromides in the aqueous phase is further investigated, since individual polybromides are involved in equilibrium Eqn. (4) and shown in Fig. 3b. For the three electrolyte series, three polybromides (Br_3^-, Br_5^- and Br_7^-) are observed. Raman spectra are shown in the ESI in Figure S-2 to S-4.

Br_2 is distributed among the individual polybromides Br_3^-, Br_5^- and Br_7^- and the distribution only slightly depends on the excess amount of bromine and the SoC in series no. 1 to 3 (Fig. 3b). Mainly no correlation between the bromine excess and the distribution is detected. Following these observations, Br_2 is distributed among the different polybromides in constant proportion and predominantly present in Br_5^- in the aqueous solution, followed by Br_3^-, while the smallest fraction of Br_2 is stored in Br_7^-. This is in accordance with observations on pure $HBr/Br_2/H_2O$-electrolytes for low absolute Br_2 concentrations [27]. Due to nearly independent polybromide distribution an influence of the polybromide distribution on further parameters cannot be investigated.

3.3. *Storage of Br_2 in the fused salt phase*

As the concentrations of Br_2 in the aqueous phase are low compared to the absolute Br_2 concentration, Br_2 is transferred in majority to the fused salt. In order to gain deeper knowledge about the mechanisms of bromine transfer, the concentration of Br_2(fs) and the distribution of Br_2 among the individual polybromides in the fused salt phase are considered. Results are shown in Fig. 4.

3.3.1. *Br_2 concentration and storage capacity in the fused salt phase*

The fused salt phase acts as the actual bromine reservoir and energy storage media as Br_2 is present in the fused salt phase at a fraction >74 mol% (Table 2). Due to the transfer of Br_2 and $[C2Py]^+$ into the fused salt (Eqn. (4)), high concentrations of both components are reached, as shown for Br_2 in Fig. 4a. Concentrations of Br_2 in the fused salt between $9.26 \leq c(Br_2\ (fs)) \leq 15.11$ M are rather high compared to those in aqueous electrolytes (Fig. 3a) and even higher than absolute Br_2 concentrations (Fig. 1a). Concentrations of Br_2 in the fused salt tend to increase for all series no. 1 to 3 with rising SoC as observed in Fig. 4a. High concentrations of Br_2 are reached in the fused salt phase due to the absence of water [11]. The fused salt is a anhydrous ionic liquid consisting of a mixture of $[C2Py]^+$ cations and polybromides [11]. Raman spectroscopy showed the existence of these three polybromides.

Due to concentrations of Br_2 in fused salts larger than 10 M Br_2 theoretically, capacities larger than 536 Ah L^{-1} are achieved related purely to the fused salt volume.

Table 2
Maximum bromine concentrations $c(Br_2,aq)_{max}$ in aqueous electrolytes including related SoC values for all three electrolyte series no. 1 to 3, as well as the fraction of bromine bound in the fused salt.

Electrolyte series	SoC of the maximum Br_2 (aq) concentration/%	Maximum concentration of $Br_2(aq)_{max}$/mM	Absolute concentration of Br_2 in sample for Br_2 $(aq)_{max}$/M	Fraction of Br_2 in fused salt compared to the absolute Br_2 concentration at SoC of $Br_2(aq)_{max}$
Series no. 1	90	277	3.015	0.908
Series no. 2	80	911	4.360	0.791
Series no. 3	70	1255	4.855	0.742

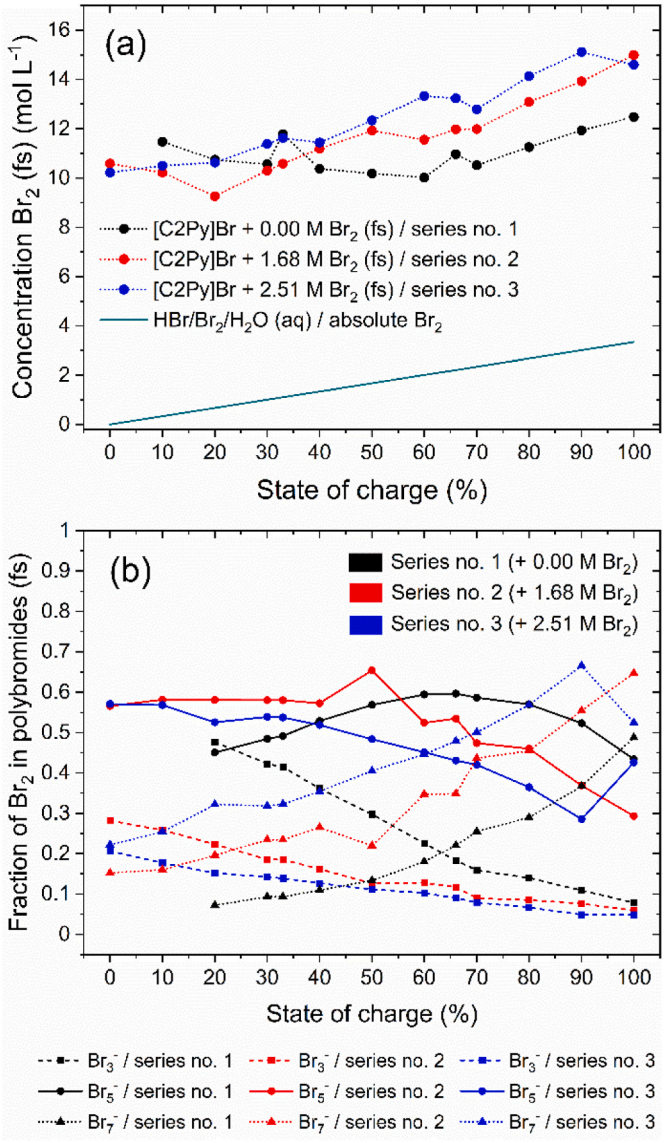

Fig. 4. Br_2 composition in the fused salt: (a) the concentration of Br_2 (fs) and (b) the Br_2 distribution on the polybromides Br_3^-, Br_5^- and Br_7^-, depending on the SoC and on the electrolyte series no. 1 to 3 investigated at $\vartheta = 23 \pm 1$ °C.

3.3.2. *Distribution of Br_2 among polybromides*

The existing polybromides in the fused salt phase are increasingly enriched by Br_2 with rising SoC as can be seen from distribution of Br_2 on the polybromides in the fused salt (Fig. 4b). The increasing Br_2 concentration in the fused salt leads to varying distribution of bromine in polybromides, resulting in an increase of higher polybromide amounts from Br_3^- to Br_5^- to Br_7^-. For all fused salt phases, a strong increase of Br_2 fraction in Br_7^- along the SoC is identified in Fig. 4b, while the fraction of Br_2 stored in Br_3^- decreases continuously. In general, with rising excess amounts of Br_2, fractions of Br_2 in Br_7^- get larger and of Br_2 in Br_3^- are lower in the fused salt in series no. 1, 2 and 3 and with rising SoC. Br_2 fraction in Br_5^- for series no. 1 rises till SoC 66% and decreases after. In electrolyte series no. 2 and 3, the fraction of Br_2 in Br_5^- stays from 0 ≤ SoC ≤40% at a value in the range from 51 to 58 mol% and decrease for SoC >40%. At SoC 100% the higher the excess amount of Br_2 in series no. 1, 2 and 3 the lower the fraction of Br_2 complexed in Br_5^-. When an excess amount of Br_2 is used, from SoC 0% onwards, there is already enough Br_2 stored in the fused salt to identify large fractions of Br_5^- and Br_7^-.

The fused salt polybromides take up Br_2 by forming higher polybromides with increasing absolute Br_2 concentrations, leading to a storage media of high capacity.

3.4. *Transfer mechanisms of bromine between aqueous phase and fused salt phase*

The transfer of bromine between the aqueous phase and the fused salt phase has been described so far with the solubility equilibrium Eqn. (4), while polybromides and $[C2Py]^+$ cations form micelles, which collapse and form a second phase during charge operation. For SoC >70% a further solubility limitation (Eqn. (9)) is introduced. In parallel to these two mechanisms, a further transfer mechanism for Br_2 into the fused salt and vice versa exists, by considering the concentration of Br_2 in the aqueous phase (Fig. 3a), the concentration of $[C2Py]^+$ in the aqueous phase (Fig. 2) and the Br_2 distribution among the polybromides in the fused salt phase (Fig. 4b):

For series no. 2 and no. 3 within the whole SoC range and for series no.1 for SoC ≥60% almost 95 mol% of the $[C2Py]^+$ are stored in the fused salt, while the aqueous phase is almost free of $[C2Py]^+$ cations. Following Eqn. (4), the existence of $[C2Py]^+$ in the aqueous phase is essential to form $[C2Py]Br_{2n+1}$(fs) salt, but $[C2Py]^+$ cations are not available in sufficient amounts in the aqueous phase (Fig. 2). Fused salts of series no. 2 and 3 are expected only rarely to absorb Br_2 from SoC ≥40% following Eqn. (4). In parallel, the actual bromine concentration in the aqueous phase increases with rising SoC (Fig. 3a), but is stoichiometrically too low, compared to the expected increase of absolute bromine (Fig. 1a). Therefore, Br_2 needs still to be absorbed by the fused salt either when $[C2Py]^+$(aq) is absent. In the fused salt, with rising SoC and absolute Br_2 concentration more Br_5^- and Br_7^- are formed (Fig. 4b). Therefore, Br_2 still passes the liquid-liquid interface between the two different electrolyte phases. A further transfer mechanism of Br_2 is proposed, which is independent of $[C2Py]^+$(aq) cations and is compared to the mechanism in Eqn. (4).

3.4.1. *Two main bromine transfer mechanisms*

Next to the solubility limit shown in Eqn. (9), two main types of bromine transfer mechanism (mechanism I and II) between the two phases appear. Both mechanisms are described in Table 3. Mechanism I characterizes the transfer of the polybromide salt into the fused salt phase and vice versa caused by its low solubility (Eqn. (4)) in the aqueous phase (Table 3/column 1), which has been investigated in the literature for Zn/Br_2-RFB electrolytes [12,15].

Mechanism II describes a transfer of Br_2 at the phase interface between the aqueous and the fused salt phase (Table 3/column 2). This mechanism bases on an exchange of Br_2 between two polybromide species existing on both sides of the liquid-liquid interface and without transfer of $[C2Py]^+$ across the interface into the aqueous phase. Driving force of this transfer is the larger solubility of Br_2 in the fused salt phase in the form of higher polybromides Br_5^- and Br_7^- [11], compared to their solubility in the aqueous phase. In mechanism II bromine is available in both phases in the form of polybromides. Low amounts of molecular Br_2(aq) are negligible [27,73]. Negatively charged polybromides cannot pass the interface without a positive charged counter ion to keep the amount of charges balanced. It is supposed that only a Br_2 molecule passes through the interface. For example, one Br_5^-(aq) molecule of the aqueous phase at the interface releases one Br_2 molecule to a Br_5^-(fs) molecule at the fused salt side interface. The Br_5^-(aq) in the aqueous phase becomes Br_3^-(aq), while the Br_5^-(fs) in the fused salt becomes Br_7^-(fs). This is confirmed by the distribution of Br_2 on the polybromides in the fused salt (Fig. 4b). Mechanism II is shown in Eqn. (10) with x = 1,2 or 3 and n = 2, 3 describing the polybromides in the different phases.

$$Br_{2x+1}^-(aq) + Br_{2n-1}^-(fs) \leftrightarrows Br_{2x-1}^-(aq) + Br_{2n+1}^-(fs) \quad (10)$$

Both transfer mechanisms I and II in Table 3 are reversible and take place in parallel along the SoC range. The presence of one or both

Table 3
Description of the possibly existing mechanisms of Br_2 transfer between the aqueous electrolyte phase and the fused salt phase, including criteria for the appearance of the individual mechanisms and effects on operation in a bromine half cell.

	Mechanism I	Mechanism II
Mechanisms		
Mechanism of Br_2 transfer between aqueous phase and fused salt phase [a]	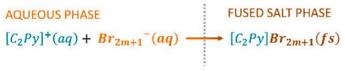	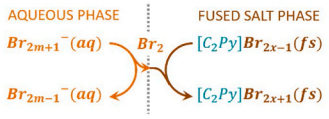
	Solubility limitation of [C2Py]Br_{2n+1} in aqueous phase	Solubility of Br_2 as polybromides in the fused salt
	[a] Br_2 transfer of electrochemical charge operation, with rising Br_2 concentrations. Dotted lines represent phase interface between aqueous phase and fused salt.	
Conditions		
c($[BCA]^+$) (aq)	c($[BCA]^+$(aq)) > 0 M	c($[BCA]^+$(aq) = 0 M
$c(Br_2)_{absolute}$	$c(Br_2)$ = 0 M at SoC 0 %	$c(Br_2)$ >> 0 M at SoC 0 %
Br_2 retention parameter	$\frac{n(Br_{2,\ absolute})}{n([C2Py]Br_{absolute})} \lesssim 2.4$	$\frac{n(Br_{2,\ absolute})}{n([C2Py]Br_{absolute})} \gtrsim 2.4$
Influence on cell operation		
Cell and scheme of bromine half cell operation for charge process operation	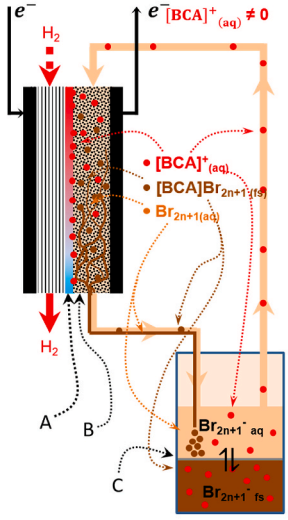	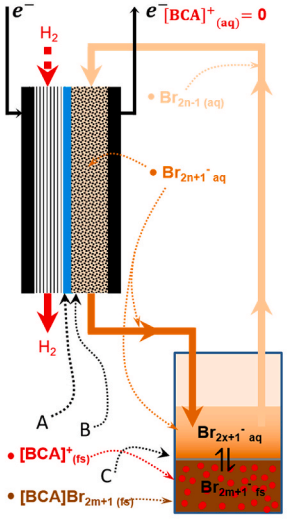
Description of influencing physical or chemical phenomena	A) PFSA membrane with low conductivity due to its interaction with $[BCA]^+$ cations, B) Formation of poorly conductive fused salt during charge process in bromine half cell and transport out of the cell to fused salt phase, C) Phase interface between aqueous phase and fused salt at which Br_2 and $[BCA]^+$ are released during discharge operation and [BCA]Br_{2n+1} is absorbed during charge operation.	A) PFSA membrane with high conductivity, B) Aqueous Br_2/Br^- posolyte without $[BCA]^+$ cations, C) Phase interface between aqueous electrolyte solution and fused salt at which bromine transfer between the polybromide phases takes place.

transfer mechanisms depends on the SoC and the excess amount of Br_2. As long as $[C2Py]^+$ exists in parallel to polybromides in aqueous solution, mechanism I is present to form fused salt (Eqn. (4)). When the SoC rises or excess amounts of Br_2 are available in the electrolyte, $[C2Py]^+$(aq) is transported with Br_2 into the fused salt phase (series no. 1 for SoC <30%). For low $[C2Py]^+$(aq) concentrations mechanisms I and II exist in parallel. Br_2 is transferred between the phases as [C2Py]Br_{2n+1} and as Br_2 at the liquid-liquid interface (series no. 1 for SoC ≈20–60% and for series no. 2 and 3 below SoC 30%). Without $[C2Py]^+$ in the aqueous solution, only mechanism II is responsible for the Br_2 transfer (series no. 2 and 3 for SoC ≥30 and 10% and in series no. 1 for SoC ≥70%).

3.4.2. *Application oriented preparation of BCA containing electrolytes*

The amount of $[C2Py]^+$ present in the aqueous solution influences the predominating transfer mechanism of Br_2 and should be as small as possible to gain high cycling capacity ranges. When approx. 95 mol% of $[C2Py]^+$ cations are stored in the fused salt phase, we assume that the transfer of Br_2 by mechanism II predominates and expect cycling is possible with only limited influence of $[C2Py]^+$(aq) cations on the cell performance. For simple preparation of electrolytes by electrolyte producers and battery operators, a concentration based parameter R is

introduced (Eqn. (11)).

Eqn. (11)) defines the electrolyte mixture for a BCA-retention in the fused salt of at least 95 mol%. From the presented concentration of $[C2Py]^+$(aq) in series 2 and 3 (Fig. 2), it can be defined, that the proportion between the absolute amount of Br_2 $n(Br_{2,absolute})$ and the absolute amount of $[BCA]^+$ cations $n([BCA]^+_{,\ absolute})$ is R. The BCA-retention parameter R is defined in Eqn. (11):

$$R = \frac{n(Br_{2,\ absolute})}{n([C2Py]Br_{\ absolute})} \tag{11}$$

In series no. 2 for SoC ≥30% and series no. 3 for SoC ≥5% less than 5 mol% of $[C2Py]^+$ are dissolved in the aqueous electrolyte leading to R = 2.41 (series no. 2 and 3). R should be higher than R ≥ 2.4, when working with an excess of bromine and the ambition of achieving a high useable electrolyte capacity.

Battery performance with improved electrolyte mixtures no. 2 and 3 is evaluated in Section 3.6 in order to validate the criterion of R ≥ 2.4.

3.5. Electrolytic conductivity of the aqueous phases

Due to fast electrochemical reaction kinetics in both half cells, high current densities in the cell are feasible [3,74], requiring high electrolyte conductivities during cell operation. Due to the low conductivity of the fused salt [15,18], only the aqueous phase is applicable. The electrolyte conductivities are investigated for all aqueous electrolytes at ϑ = 23 ± 1 °C and are compared in Fig. 5. In addition, conductivities of pure HBr/H_2O electrolytes [75] (orange line) and of BCA-free $HBr/Br_2/H_2O$ posolytes [27] (green line) are depicted in Fig. 5.

High conductivities between 344.9 ≤ κ ≤ 781.2 mS cm^{-1} are measured across all SoCs and aqueous electrolyte series (Fig. 5). High proton concentrations in aqueous solution with $c(H^+) \geq 1$ M lead to high conductivity values by means of the Grotthus mechanism [76,77]. The conductivities of series no. 2 and 3 correspond approximately to the conductivity values of pure HBr/H_2O solutions at ϑ = 20 °C and reach a maximum conductivity due to the excess amount of bromine within the whole SoC range compared to series no. 1.

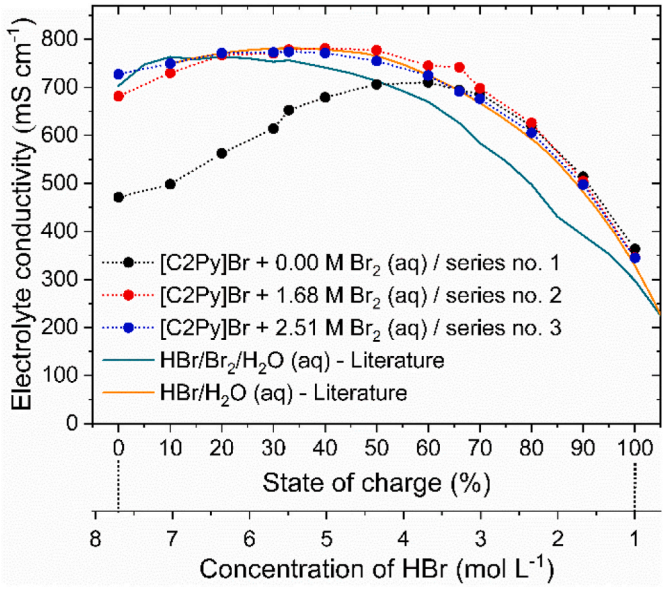

Fig. 5. Electrolyte conductivity of the aqueous electrolyte phase depending on SoC/HBr concentration and electrolyte series (no. 1 - black, no. 2 - red, no. 3 - blue) and conductivity of the BCA-free electrolyte $HBr/Br_2/H_2O$ without an excess of Br_2 (+0.00 M Br_2) (green line) from literature [27] (all at ϑ = 23 ± 1 °C), as well as comparison with bromine-free and BCA-free, pure HBr/H_2O solutions converted to the SoC scale (orange line) from literature (ϑ = 20 °C) [75]. (For interpretation of the references to colour in this figure legend, the reader is referred to the Web version of this article.)

For SoC ≤66% there is a strong difference in conductivities between electrolyte no. 1 and series no. 2 and 3. The presence of large organic $[C2Py]^+$ cations in series no. 1 (κ = 471.3 mS cm^{-1}, SoC 0%) decreases the conductivity strongly, while conductivities of the nearly BCA-free aqueous phases of series no. 2 (κ = 681.7 mS cm^{-1}, SoC 0%) and no. 3 (κ = 727.2 mS cm^{-1}, SoC 0%) remain at high values. The mobility of the organic cation is limited due to its larger hydrodynamic radius. In addition, charge transport by means of the Grotthus mechanism needs to bypass the larger cations. As the aqueous phases of series no. 2 and 3 are nearly BCA-free within the whole SoC range, maximum conductivities independent of the BCA are reached. The excess of Br_2 and rising Br_2 concentrations over the SoC result in an increased transfer of $[C2Py]^+$ in the fused salt phase and lead to higher conductivities of the aqueous phase.

For SoC ≥66% the conductivity of all electrolytes in series no. 1 to 3 decreases, in accordance with the values in literature [11,27], and is independent of the amount of excess Br_2. The proton concentration decreases to 1 M at SoC 100% due to the cell reaction, leading to a falling conductivity. Since $[C2Py]^+$ cations are not present in the aqueous electrolyte in this SoC range, they do not influence the conductivity. But as $[C2Py]^+$ cations bind large amounts of Br_2 in the fused salt phase, they reduce the amount of polybromides in the aqueous phase. The conductivity in aqueous solution is increased compared to BCA-free $HBr/Br_2/H_2O$ electrolyte (Fig. 5 – green line), as the Grotthus mechanism of protons is rarely influenced by polybromides.

The modification of the electrolytes by adding Br_2 at SoC 0% is of high interest for cell application due to rising conductivities in series no. 2 and 3 within the entire SoC range.

3.6. Cell performance

3.6.1. Characteristic cycling voltages and useable electrolyte capacities

Galvanostatic cycling tests for all electrolytes are performed in the H_2/Br_2-RFB single cell at ±50 mA cm^{-2}. Cell voltages, positive half-cell potentials and redox potentials are presented in Fig. 6.

For series no. 1 without Br_2 excess, there is a strong influence of the $[C2Py]^+$ cations on the cell performance (Fig. 6a). During charge, a strong voltage peak is present and during discharge, the voltage decreases strongly, so that the lower voltage limit is reached rapidly and a maximum range between SoC 100% and SoC 63% can be cycled. Only a maximum of 37% of the capacity can be used. This is in agreement with results from Ref. [18]. The $[C2Py]^+$ cations lead to the formation of poorly conducting fused salt in the bromine half cell during charge and interact with the Nafion117 during discharge, resulting in high overvoltages.

By adding Br_2 to series no. 2 and 3, the both adverse effects of $[C2Py]^+$ cations on cell performance are largely limited for cycling of series no. 2 (Fig. 6b) and nearly eliminated for series no. 3 (Fig. 6c). In both cases $[C2Py]^+$ cations are mainly stored in the fused salt (Fig. 2) and therefore their drawbacks on cell performance are diminished (Table 3/mechanism II). From cell tests it is investigated, that for both electrolyte series it is possible to carry out complete discharge and charge cycles within the selected SoC range, starting from electrolytes with a SoC 100%. A useable capacity of 179.6 Ah L^{-1} is achieved for the first time for this type of battery using a BCA for Br_2 complexation in the electrolyte and a PFSA based Nafion117 membrane.

For electrolyte series no. 2, complete discharge and charge cycles in the SoC range can be achieved, but still a strong influence of the $[C2Py]^+$(aq) cations is evident (Fig. 6b) during charging process. An increase in cell voltage forms a peak, then flattens out again and demonstrates the presence of small amounts of $[C2Py]^+$ cations in the aqueous phase. In combination fused salt is formed in the electrode felt and causes an overvoltage in the half cell. The formation of fused salt is available but does not limit the useable electrolyte capacity. The small but rapid voltage and potential fluctuations in Fig. 6 are due to an air

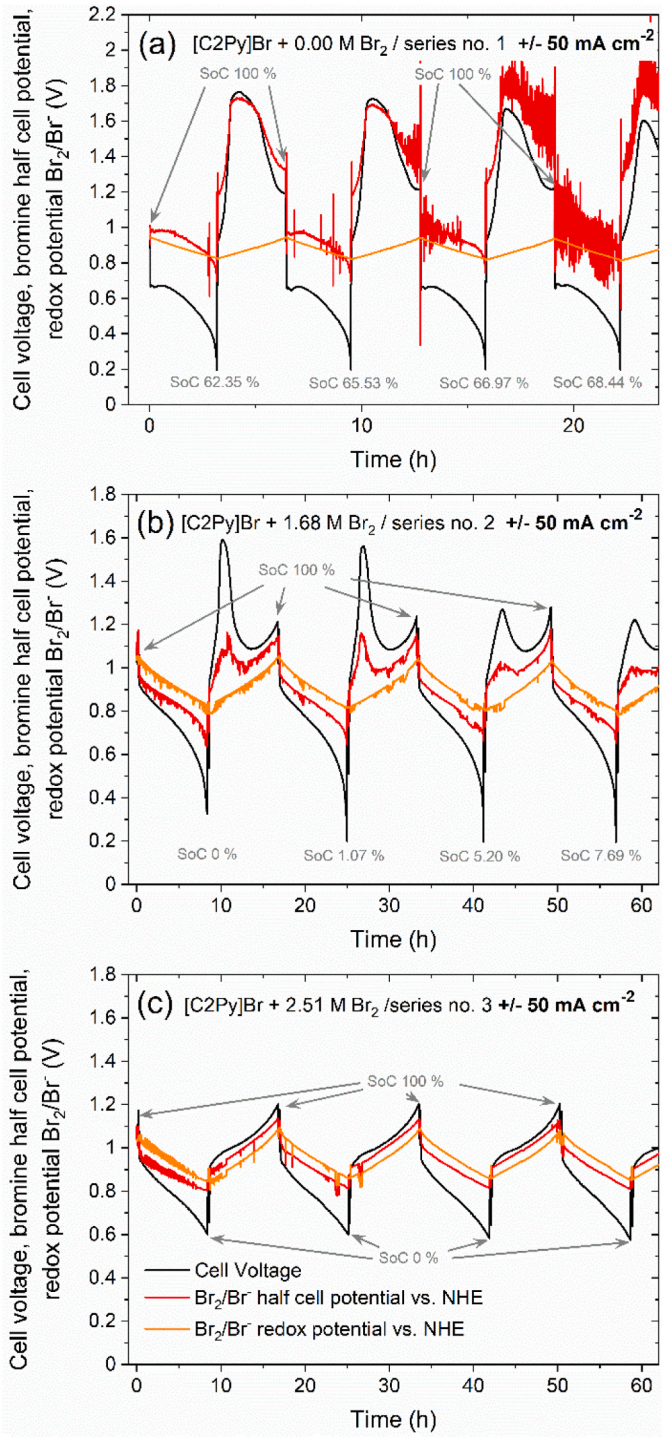

Fig. 6. Cell voltage, positive bromine half cell potential vs. NHE and redox potential of the bromine/bromide electrolyte vs. NHE for electrolyte series (a) no 1 (+0.00 M Br_2), (b) no. 2 (+1.68 M Br_2) and (c) no. 3 (+2.51 M Br_2) for galvanostatic cycling with i = ±50 mA cm^{-2} in a 40 cm^2 H_2/Br_2-RFB single cell within thresholds between +3.0 and 0.2 V. In grey letters maximum SoC values before discharge operation and minium SoC values after discharge operation are shown for the cycling tests in (a–c).

bubble or a drop of fused salt in front of the ceramic frit of the reference electrode. However, the general trend and the statements remain unaffected.

Results of cycling test with electrolyte series no. 3 (Fig. 6b) are only slightly effected by low concentrated $[C2Py]^+$ cations as more than 95% of the $[C2Py]^+$ cations are bound in the fused salt phase. The shape of cell voltage curve is similar with the voltage trends of BCA-free electrolytes from literature [27,78]. Due to the low amount of $[C2Py]^+$(aq) in the half cell the formation of low conductive fused salt is supressed. As no overvoltage is caused during charge, the cell voltage does not tend to show a peak. During discharge the cell voltage decreases stronger than the bromine half-cell potential, but ends at high values of 0.6 V. Full discharge of 179.6 Ah L^{-1} is reached. The redox potential of the Br_2/Br^- electrolyte is in parallel to the bromine half cell potential during charge and discharge.

Since at SoC 0% for series no. 2 and 3 there are concentrations of bromine of 0.24 M and 0.44 M, respectively, no mass transport limitation in the bromine half cell occurs during the discharge process when approaching SoC 0%. This is evident by the bromine half-cell potential, that does not decrease while the cell voltage decreases strongly (red vs. black lines in Fig. 6b and c).

Energy efficiency (EE) for the first three cycles of electrolytes of series no. 2 (EE = 60.0%) are lower than for series no. 3 (EE = 74.5%) due to the effects of $[C2Py]^+$ in the bromine half cell. In series no. 1 the $[C2Py]^+$ cations have highest effect leading to a low EE = 39.5%. The fused salt caused in series no. 2 by higher $[C2Py]^+$ causes the voltage peak due to its low conductivity based overvoltage, leading to lower EE in this test. An excess of +2.51 M Br_2 to the electrolyte in series no. 3 leads to stable and performant cycles.

3.6.2. *Membrane performance*

In order to determine the influence of $[C2Py]^+$ cations in the electrolytes on the membrane resistance, which is part of the ohmic cell resistance, the ohmic cell resistance of the cell before and after the discharge process is investigated using EIS and shown in Fig. 7. Before the first cycle the ohmic cell resistance R_{OHM} is 1.10–1.25 Ω cm^2 in all cells. For all cell tests with different electrolyte series, R_{OHM} is higher

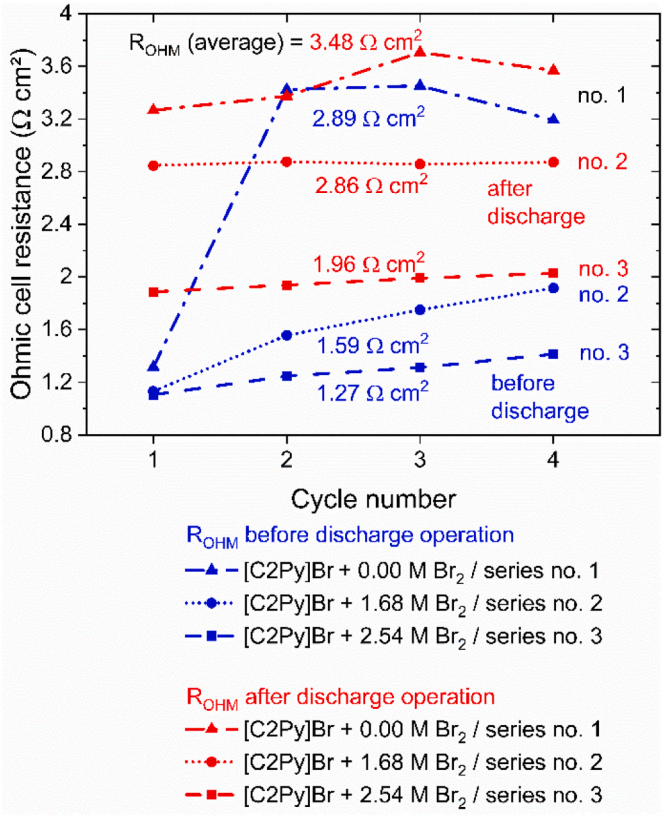

Fig. 7. Ohmic cell resistance R_{OHM} of the investigated H_2/Br_2-RFB single cell before and after discharge operation in cycling tests for electrolyte series no.1, 2 and 3 depending on the cycle number of both, determined by electrochemical impedance spectroscopy during cell cycling experiment in Fig. 6a–c.

after discharge. From this results it is expected, that during discharge $[C2Py]^+$ is released from fused salt into the aqueous phase and interacts with the PFSA membrane [18]: An average value for R_{OHM} after discharge operation of $R_{OHM} = 3.48\ \Omega\ cm^2$ (series no. 1), $R_{OHM} = 2.86\ \Omega\ cm^2$ (series no. 2) and $R_{OHM} = 1.96\ \Omega\ cm^2$ (series no. 3) is calculated from values in Fig. 7. Although all series show an increased ohmic cell resistance, this effect strongly depends on the selected series. During discharge, higher concentrations of $[C2Py]^+$ are available for series no. 1 and no. 2, while for series no. 3 less than 0.07 M [C2Py]Br are dissolved in aqueous solution. As the electrolyte conductivity is high for discharged electrolytes at SoC 0% (Fig. 5) and the ohmic cell resistances of further cell materials are assumed to be constant, the rise in cell resistance is most probably associated with the reduced conductivity of the Nafion117 membrane in contact with $[C2Py]^+$ cations. The interaction of the cations with the membrane is not reversible during charge [18].

Even low amounts of large organic $[C2Py]^+$ cations in solution interact with the sulphonate groups of the Nafion117 membrane, forming an addition bonding and hindering the transport of protons and water through the membrane structure [43,79]. This phenomenon in the H_2/Br_2-RFB is described in detail in Refs. [17,18]. The organic $[C2Py]^+$ cation dries the membrane of water by forming hydrophobic spaces in its porous structure [79]. The membrane conductivity decreases, and R_{OHM} rises, as shown in Fig. 7.

3.6.3. *Efficiencies for long-term cycling and different current densities*

In order to test the stability of the electrolytes, long-term cycling tests are performed for electrolytes no. 2 and 3 at a current density of ±100 mA cm^{-2}. Cell voltage and mass change of the bromine electrolyte are recorded (Fig. 8a+b). Long term cycling of series 1 was carried out and discussed in detail in Ref. [18].

The long term cycling is performed for 9 cycles only, as the mass of electrolyte decreases strongly during the tests (Fig. 8/a-b). The mass of the electrolyte decreases independently of the electrolyte series by approximately 40 g (29.8%) throughout 9 cycles. At the outlet of the hydrogen half cell, clear but strongly acidic liquid is collected from the cell in a washing bottle. There is a strong crossover of the individual components. This is mainly caused by a crossover of water and Br_2 into the hydrogen half cell such as has been determined for series no. 1 in Ref. [18]. The crossover leads in parallel to an intense release of Br_2 and $[C2Py]^+$ cations from the fused salt into the aqueous phase [18]. Thus, the lack of Br_2 in the aqueous electrolyte caused by the crossover of Br_2 into the hydrogen half cell is compensated. Simultaneously, $[C2Py]^+$ cations are released and diffuse into the PFSA membrane and interact with the sulphonate groups. The membrane conductivity is reduced with increasing cycle number by an increasing release of $[C2Py]^+$. Ohmic cell resistances rise due to rising membrane resistances.

For series no. 2, the release of $[C2Py]^+$ from the fused salt at ±100 mA cm^{-2} and the interaction with the Nafion117 membrane lead to strongly increasing ohmic cell resistances and in the discharge process the lower voltage threshold is reached without reaching the complete electrolyte to be discharged (Fig. 8a). For the selected current density, the minimum SoC continues to increase after discharge (Fig. 8a). A complete discharge and thus a cycling of the capacity of 179.6 Ah L^{-1} is not possible. This effect is intensified by the crossover or mass loss of the electrolyte. For series no. 3 a complete discharge operation is possible within the first four cycles. For the further cycles, the same effect occurs as for series no. 2, but with a delay and with higher depths of discharge (Fig. 8b).

For the application of this idea using an access amount of Br_2, it is therefore necessary to use stronger BCAs which are bind more strongly in the fused salt even when Br_2 is released from the fused salt. For

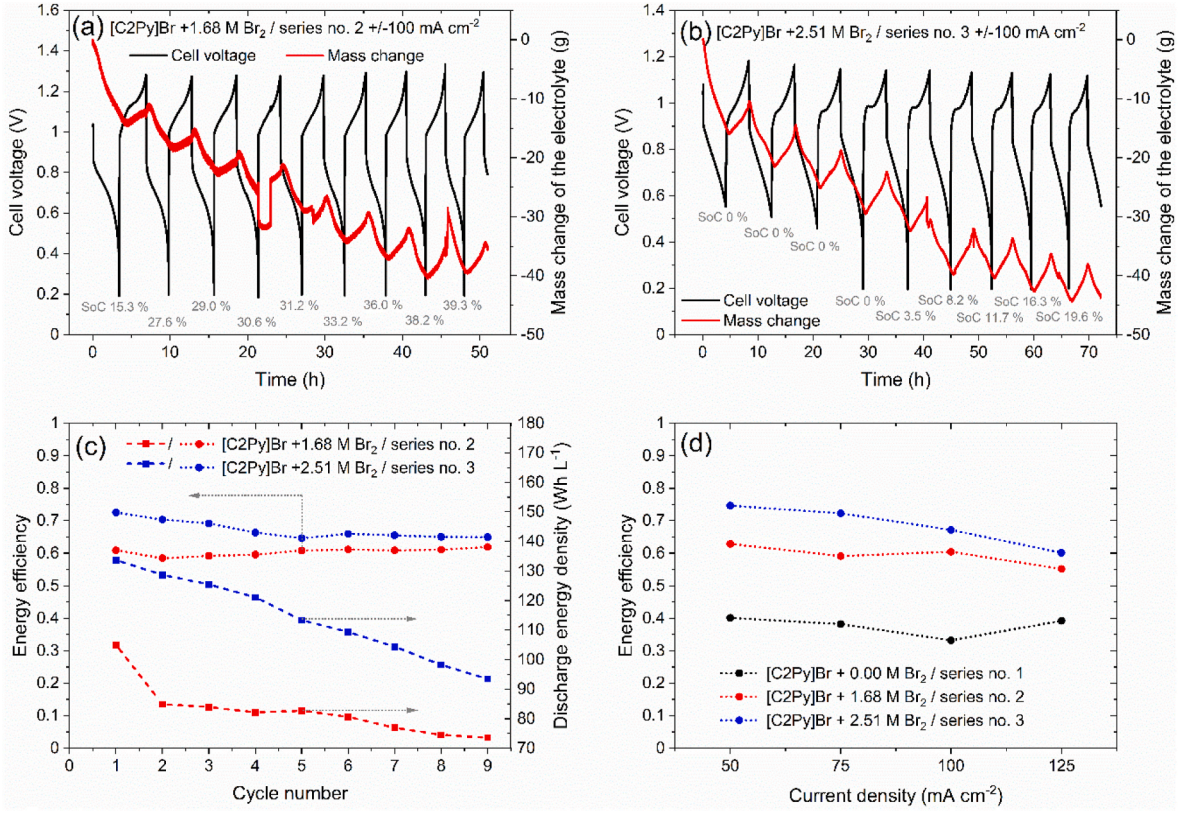

Fig. 8. Long-term cycling of electrolytes (a) series no. 2 and (b) series no. 3 by galvanostatic cycling at ±100 mA cm^{-2} (cell voltage and mass change of the bromine electrolyte). From the long-term cycling, (c) energy efficiencies of the individual cycles and (c) discharge energy densities related to the electrolyte volume are calculated depending on each cycle number. Further, (d) energy efficiencies of series 1, 2 and 3 at different current densities, each for the 2nd cycle at the corresponding current density are shown.

example, [C2Py]Br could be replaced by 1-*n*-hexylpyridin-1-ium bromide, which is stronger interacting with polybromides [11]. However, the crossover must be reduced in later experiments by higher pressures of the hydrogen gas in the hydrogen anode.

Despite strongly decreasing useable capacities, the energy efficiencies of the battery remain relatively constant (58.5–61.9% for series no. 2 and 64.6–72.5% for series no. 3 in Fig. 8c). However, the efficiencies are not very meaningful, as they remain essentially constant for each series. In contrast, the amounts of energy discharged during the discharge process (Fig. 8c) for the different series are significant. They decrease due to the decreasing useable capacities (Fig. 8c). However, the excess bromine in series no. 3 improves the discharge energy density (93–133 Wh L^{-1}) compared to series no. 2. However, due to the increasing influence of the $[C2Py]^+$ cations, the discharge energy density decreases strongly within the 9 cycles.

Furthermore, energy efficiencies for all electrolytes are investigated at higher current densities (±50, ±75, ±100 and ± 125 mA cm^{-2}) and are measured in the 2nd cycle in each case. The EE (Fig. 8d) for series no. 1 ($40.1 \geq EE \geq 33.2\%$), series no. 2 ($62.9 \geq EE \geq 55.2\%$) and series no. 3 ($74.7 \geq EE \geq 60.1\%$) increase with increasing excess amounts of Br_2, suggesting better energy efficiency in aqueous $[C2Py]^+$-free series no. 2 and 3. With increasing current density, the energy efficiencies decrease slightly (Fig. 8d). Based on the results in sections 3.1 to 3.6.3 and in Ref. [18] we suggest the following explanation: The slight decrease in EE is attributed to the higher overvoltages of the ohmic cell resistance of the cell at higher current densities. On the one hand (1) the current in the cell increases, which leads to higher overvoltages and at the same time (2) the ohmic resistance increases due to the release of $[C2Py]^+$ cations. For higher discharge currents Br_2 is consumed faster in the positive half cell and a faster release of Br_2 from the fused salt into the aqueous phase is expected, causing also an increased transfer of higher amounts of $[C2Py]^+$. Higher concentrations of $[C2Py]^+$ in the aqueous phase can interact with the membrane. Charge and discharge times for higher currents shorten and thus the useable capacities. In series no. 1, mass transport inhibition due to a lack of Br_2 in front of the electrode as a limiting step predominates with increasing current density, while for series no. 2 and 3, the ohmic resistances of the cell and membrane as a limiting step predominate for the current densities investigated.

4. Conclusions

The selective investigation of the bromine electrolyte with BCAs using the example of [C2Py]Br allowed the development of safe and efficient electrolytes for bromine half cells in H_2/Br_2-RFB. By adding an excess amount of Br_2 it is possible to actively interfere into the BCA-solubility equilibrium in order transfer large parts (>95 mol%) of the $[C2Py]^+$ from the aqueous phase into the second available fused salt phase and to bind it there.

By focusing on the distribution of Br_2 in the fused salt polybromides and the concentration of $[C2Py]^+$ and Br_2 in the aqueous phase, it was found that a transfer of Br_2 happens in an absorption process at the liquid-liquid interface. When $[C2Py]^+$(aq) is absent, in a second transfer mechanism only Br_2 was transferred from a polybromide in the aqueous phase to a polybromide in the fused salt phase. By adding an excess of Br_2, the transfer by solubility limitation of the fused salt is suppressed, while the transfer mechanism without $[C2Py]^+$ allowed the transfer of Br_2 between the phases.

The adverse effects of formation of fused salt in the cell and low conductivities of the PFSA membranes in contact with organic $[C2Py]^+$ cations are reduced or eliminated, while Br_2 is still stored safely in the fused salt. While earlier measurements without the modification of the electrolyte showed limited cell performance and a useable capacity of only 53.9 Ah L^{-1}, with this approach, a useable capacity of 179.6 Ah L^{-1} is achieved for the first time including the application of a BCA and a PFSA membrane. Crossover of the electrolyte leads to reduction of this capacity. Despite a significant reduction of $[BCA]^+$ content in the aqueous phase, small amount of it remained dissolved, which lowers the membrane conductivity.

For future investigation, a stronger BCA than [C2Py]Br should be combined with excess amounts of Br_2 in the electrolytes to reduce both, Br_2 to moderate concentrations and transfer $[BCA]^+$ cations completely to the fused salt phase. Also a focus should be to develop a cell design to operate the cell with aqueous electrolytes at higher current densities and lower electrolyte crossover during cycling.

CRediT authorship contribution statement

Michael Küttinger: Conceptualization, Methodology, Investigation, Formal analysis, Visualization, Writing – original draft, Writing – review & editing, Funding acquisition, Project administration, Supervision. **Raphaël Riasse:** Investigation, Formal analysis, Visualization. **Jakub Wlodarczyk:** Formal analysis, Writing – review & editing. **Peter Fischer:** Writing – review & editing. **Jens Tübke:** Resources.

Declaration of competing interest

The authors declare that they have no known competing financial interests or personal relationships that could have appeared to influence the work reported in this paper.

Acknowledgements

We acknowledge for funding of Federal Ministry of Education and Research BMBF within the framework of a German-Israeli research ("PEDUSA") with project number 03XP0135 and by the European Union's Horizon 2020 research programme (Agreement no. 765289).

Appendix A. Supplementary data

Supplementary data to this article can be found online at https://doi.org/10.1016/j.jpowsour.2021.230804.

References

[1] Y.A. Hugo, W. Kout, G. Dalessi, A. Forner-Cuenca, Z. Borneman, K. Nijmeijer, Processes 8 (2020) 1492, https://doi.org/10.3390/pr8111492.
[2] J. Noack, N. Roznyatovskaya, T. Herr, P. Fischer, Angew. Chem. Int. Ed. 54 (2015) 9776–9809, https://doi.org/10.1002/anie.201410823.
[3] K.T. Cho, M.C. Tucker, A.Z. Weber, Energy Technol. 4 (2016) 655–678, https://doi.org/10.1002/ente.201500449.
[4] Y.V. Tolmachev, Russ. J. Electrochem. 50 (2014) 301–316, https://doi.org/10.1134/S1023193513120069.
[5] K.T. Cho, M.C. Tucker, M. Ding, P. Ridgway, V.S. Battaglia, V. Srinivasan, A. Z. Weber, ChemPlusChem 80 (2015) 402–411, https://doi.org/10.1002/cplu.201402043.
[6] W. Glass, G.H. Boyle, Fuel Cell Systems: Performance of Hydrogen-Bromine Fuel Cells, American Chemistry Society, Washington D. C., 1965.
[7] A.J. Bard, R. Parsons, J. Jordan, Standard Potentials in Aqueous Solution: Bromine, CRC Press, New York, 1985.
[8] G. Jones, S. Baeckström, J. Am. Chem. Soc. 56 (1934) 1524–1528, https://doi.org/10.1021/ja01322a022.
[9] K.J. Cathro, K. Cedzynska, D.C. Constable, P.M. Hoobin, J. Power Sources 18 (1986) 349–370, https://doi.org/10.1016/0378-7753(86)80091-X.
[10] S.N. Bajpai, J. Chem. Eng. Data 26 (1981) 2–4, https://doi.org/10.1021/je00023a002.
[11] M. Küttinger, P.A. Loichet Torres, E. Meyer, P. Fischer, J. Tübke, Molecules 26 (2021) 2721, https://doi.org/10.3390/molecules26092721.
[12] E. Lancry, B.-Z. Magnes, I. Ben-David, M. Freiberg, ECS Trans 53 (2013) 107–115, https://doi.org/10.1149/05307.0107ecst.
[13] Magnes, et al., Additives for Zinc-Bromine Membraneless Flow Cells, Bromine Compounds Ltd, 2013, 09.05.13.
[14] B.-Z. Magnes, Bromine Based Rechargeable Batteries - The Chemistry and the Electrochemistry, ICL Industrial Products / Bromine compounds Ltd., Israel, 2015, pp. 1–2.
[15] D.J. Eustace, J. Electrochem. Soc. 127 (1980) 528–532, https://doi.org/10.1149/1.2129706.
[16] P.M. Hoobin, K.J. Cathro, J.O. Niere, J. Appl. Electrochem. 19 (1989) 943–945, https://doi.org/10.1007/BF01007946.
[17] K. Saadi, M. Kuettinger, P. Fischer, D. Zitoun, Energy Technol. 9 (2021) 2000978, https://doi.org/10.1002/ente.202000978.

[18] M. Küttinger, R. Brunetaud, J.K. Włodarczyk, P. Fischer, J. Tübke, J. Power Sources 495 (2021) 229820, https://doi.org/10.1016/j.jpowsour.2021.229820.
[19] W.C. Bray, J. Am. Chem. Soc. 32 (1910) 932–938, https://doi.org/10.1021/ja01926a005.
[20] F.P. Worley, J. Chem. Soc. Trans. 87 (1905) 1107–1123, https://doi.org/10.1039/CT9058701107.
[21] L. Korson, W. Drost-Hansen, F.J. Millero, J. Phys. Chem. 73 (1969) 34–39, https://doi.org/10.1021/j100721a006.
[22] D.B. Scaife, H.J.V. Tyrrell, J. Chem. Soc. (1958) 386–392, https://doi.org/10.1039/JR9580000386, 0.
[23] H.A. Liebhafsky, J. Am. Chem. Soc. 56 (1934) 1500–1505, https://doi.org/10.1021/ja01322a016.
[24] R.O. Griffith, A. McKeown, A.G. Winn, Trans. Faraday Soc. 28 (1932) 101–107, https://doi.org/10.1039/TF9322800101.
[25] G.N. Lewis, M. Randall, J. Am. Chem. Soc. 38 (1916) 2348–2356, https://doi.org/10.1021/ja02268a008.
[26] R.W. Ramette, D.A. Palmer, J. Solut. Chem. 15 (1986) 387–395, https://doi.org/10.1007/BF00646261.
[27] M. Küttinger, J.K. Wlodarczyk, D. Daubner, P. Fischer, J. Tübke, RSC Adv. 11 (2021) 5218–5229, https://doi.org/10.1039/D0RA10721B.
[28] C. Fabjan, G. Hirss, Dechema Monographien Band 102 (1985) 149–161.
[29] P.M. Hoobin, K.J. Cathro, J.O. Niere, J. Appl. Electrochem. 19 (1989) 943–945, https://doi.org/10.1007/BF01007946.
[30] D. Linden, T.B. Reddy, Handbook of Batteries, vol. 3, McGraw-Hill, New York, NY [u.a., 2002.
[31] K.J. Cathro, K. Cedzynska, D.C. Constable, J. Power Sources 16 (1985) 53–63, https://doi.org/10.1016/0378-7753(85)80003-3.
[32] W. Kautek, J. Electrochem. Soc. 146 (1999) 3211–3216, https://doi.org/10.1149/1.1392456.
[33] B.-Z. Magnes, R. Elazari, I. Ben-David, R. Costi, Int. Flow. Battery. Forum 2017 - Conf. Paper. 6 (2015) 98–99.
[34] M. Schneider, G.P. Rajarathnam, M.E. Easton, A.F. Masters, T. Maschmeyer, A. M. Vassallo, RSC Adv. 6 (2016) 110548–110556, https://doi.org/10.1039/C6RA23446A.
[35] D. Bryans, B.G. McMillan, M. Spicer, A. Wark, L. Berlouis, J. Electrochem. Soc. 164 (2017) A3342–A3348, https://doi.org/10.1149/2.1651713jes.
[36] X. Chen, M.A. Rickard, J.W. Hull, C. Zheng, A. Leugers, P. Simoncic, Inorg. Chem. 49 (2010) 8684–8689, https://doi.org/10.1021/ic100869r.
[37] G.P. Rajarathnam, M.E. Easton, M. Schneider, A.F. Masters, T. Maschmeyer, A. M. Vassallo, RSC Adv. 6 (2016) 27788–27797, https://doi.org/10.1039/C6RA03566C.
[38] M.E. Easton, A.J. Ward, B. Chan, L. Radom, A.F. Masters, T. Maschmeyer, Phys. Chem. Chem. Phys. 18 (2016) 7251–7260, https://doi.org/10.1039/c5cp06913k.
[39] N. Mazur, Y.A. Hugo, W. Kout, F. Sikkema, R. Elazari, R. Costi, Int. Flow. Battery. Forum - Con. paper. 8 (2017) 52–53.
[40] Y.A. Hugo, N. Mazur, W. Kout, F. Sikkema, Z. Borneman, K. Nijmeijer, J. Electrochem. Soc. 166 (2019) A3004–A3010, https://doi.org/10.1149/2.0951913jes.
[41] Q. Che, R. He, J. Yang, L. Feng, R.F. Savinell, Electrochem. Commun. 12 (2010) 647–649, https://doi.org/10.1016/j.elecom.2010.02.021.
[42] J. Yang, Q. Che, L. Zhou, R. He, R.F. Savinell, Electrochim. Acta 56 (2011) 5940–5946, https://doi.org/10.1016/j.electacta.2011.04.112.
[43] T. Schäfer, R.E. Di Paolo, R. Franco, J.G. Crespo, Chemical Communications, 2005, pp. 2594–2596, https://doi.org/10.1039/B501507C. Cambridge, England.
[44] M.N. Szentirmay, N.E. Prieto, C.R. Martin, J. Phys. Chem. 89 (1985) 3017–3023, https://doi.org/10.1021/j100260a013.
[45] S.V. Dzyuba, R.A. Bartsch, J. Heterocycl. Chem. 38 (2001) 265–268, https://doi.org/10.1002/jhet.5570380139.
[46] A. Aupoix, B. Pégot, G. Vo-Thanh, Tetrahedron 66 (2010) 1352–1356, https://doi.org/10.1016/j.tet.2009.11.110.
[47] P. Bonhôte, A.-P. Dias, N. Papageorgiou, K. Kalyanasundaram, M. Grätzel, Inorg. Chem. 35 (1996) 1168–1178, https://doi.org/10.1021/ic951325x.
[48] B. Schrader, W. Meier, Raman/IR Atlas Organischer Verbindungen/of Organic Compounds, Verlag Chemie, Weinheim/Bergstr., 1974.
[49] M. Fleischmann, P.J. Hendra, A.J. McQuillan, Chem. Phys. Lett. 26 (1974) 163–166, https://doi.org/10.1016/0009-2614(74)85388-1.
[50] D. Cook, Can. J. Chem. 39 (1961) 2009–2024, https://doi.org/10.1139/v61-271.
[51] W. Vielstich, Z. für Anal. Chem. 173 (1960) 84–87, https://doi.org/10.1007/BF00448719.
[52] V.G.'e. Levich, Physiochemical Hydrodynamics, Prentice-Hall, Englewood Cliffs, N.J., 1962.
[53] F. Opekar, P. Beran, J. Electroanal. Chem. Interfacial Electrochem. 69 (1976) 1–105, https://doi.org/10.1016/S0022-0728(76)80129-5.
[54] S. Treimer, A. Tang, D.C. Johnson, Electroanalysis 14 (2002) 165, https://doi.org/10.1002/1521-4109(200202)14:3<165:AID-ELAN165>3.0.CO;2-6.
[55] A.J. Bard, L.R. Faulkner, Electrochemical Methods: Fundamentals and Applications, second ed., John Wiley & Sons, Inc., United States of America, 2001.
[56] G.C. Hayward, P.J. Hendra, Spectrochim. Acta Mol. Spectros 23 (1967) 2309–2314, https://doi.org/10.1016/0584-8539(67)80124-7.
[57] J.C. Evans, Grace Y.S. Lo, Inorg. Chem. 6 (1967) 1483–1486, https://doi.org/10.1021/ic50054a011.
[58] H. Haller, J. Schröder, S. Riedel, Angew. Chem. Int. Ed. 52 (2013) 4937–4940, https://doi.org/10.1002/anie.201209928.
[59] G. Bauer, J. Drobits, C. Fabjan, H. Mikosch, P. Schuster, J. Electroanal. Chem. 427 (1997) 123–128, https://doi.org/10.1016/S0022-0728(96)04992-3.
[60] B. Jiang, L. Wu, L. Yu, X. Qiu, J. Xi, J. Membr. Sci. 510 (2016) 18–26, https://doi.org/10.1016/j.memsci.2016.03.007.
[61] B. Jiang, L. Yu, L. Wu, Di Mu, Le. Liu, J. Xi, X. Qiu, ACS Appl. Mater. Interfaces 8 (2016) 12228–12238, https://doi.org/10.1021/acsami.6b03529.
[62] R.S. Yeo, J. McBeen, J. Electrochem. Soc. 126 (1979) 1682, https://doi.org/10.1149/1.2128776.
[63] R.S. Yeo, J. McBreen, G. Kissel, F. Kulesa, S. Srinivasan, J. Appl. Electrochem. 10 (1980) 741–747, https://doi.org/10.1007/BF00611277.
[64] R.S. Baldwin, NASA Tech. Memo. 89862 (1987) 1–26.
[65] J. Noack, G. Cognard, M. Oral, M. Küttinger, N. Roznyatovskaya, K. Pinkwart, J. Tübke, J. Power Sources 326 (2016) 137–145, https://doi.org/10.1016/j.jpowsour.2016.06.121.
[66] F.T. Wandschneider, M. Küttinger, J. Noack, P. Fischer, K. Pinkwart, J. Tübke, H. Nirschl, J. Power Sources 259 (2014) 125–137, https://doi.org/10.1016/j.jpowsour.2014.02.087.
[67] N.W. DeLuca, Y.A. Elabd, J. Power Sources 163 (2006) 386–391, https://doi.org/10.1016/j.jpowsour.2006.09.009.
[68] H.-L. Lin, T.L. Yu, L.-N. Huang, L.-C. Chen, K.-S. Shen, G.-B. Jung, J. Power Sources 150 (2005) 11–19, https://doi.org/10.1016/j.jpowsour.2005.02.016.
[73] J.K. Wlodarczyk, M. Küttinger, A.K. Friedrich, J.O. Schumacher, J. Power Sources (2021) 230202, https://doi.org/10.1016/j.jpowsour.2021.230202.
[74] R.S. Yeo, D.-T. Chin, J. Electrochem. Soc. 127 (1980) 549–555, https://doi.org/10.1149/1.2129710.
[75] W.J. Hamer, H.J. DeWane, Electrolytic Conductance and the Conductances of the Halogen Acids in Water, U. S. Government Printing Office, Washington D. C., 1970.
[76] K.-D. Kreuer, A. Rabenau, W. Weppner, Angew. Chem. 94 (1982) 224–225, https://doi.org/10.1002/ange.19820940335.
[77] A.T. Howe, M.G. Shilton, J. Solid State Chem. 28 (1979) 345–361, https://doi.org/10.1016/0022-4596(79)90085-9.
[78] K.T. Cho, P. Albertus, V. Battaglia, A. Kojic, V. Srinivasan, A.Z. Weber, Energy Technol. 1 (2013) 596–608, https://doi.org/10.1002/ente.201300108.
[79] K.M. Cable, K.A. Mauritz, R.B. Moore, J. Polym. Sci., Part B: Polym. Phys. 33 (1995) 1065–1072, https://doi.org/10.1002/polb.1995.090330710.